

PKS 1424+240: yet another masquerading BL Lac object as a possible IceCube neutrino source

P. Padovani^{1,2*}, B. Boccardi³, R. Falomo⁴, P. Giommi^{5,6,7}

¹European Southern Observatory, Karl-Schwarzschild-Str. 2, D-85748 Garching bei München, Germany

²Associated to INAF - Osservatorio di Astrofisica e Scienza dello Spazio, Via Piero Gobetti 93/3, I-40129 Bologna, Italy

³Max-Planck-Institut für Radioastronomie, Auf dem Hügel 69, 53121 Bonn, Germany

⁴INAF - Osservatorio Astronomico di Padova, vicolo dell'Osservatorio 5, I-35122, Padova, Italy

⁵Associated to Agenzia Spaziale Italiana, ASI, via del Politecnico s.n.c., I-00133 Roma, Italy

⁶Institute for Advanced Study, Technische Universität München, Lichtenbergstrasse 2a, D-85748 Garching bei München, Germany

⁷Center for Astro, Particle and Planetary Physics, New York University Abu Dhabi, United Arab Emirates

Accepted XX. Received YY; in original form ZZ

ABSTRACT

We show that the blazar PKS 1424+240, which has been recently associated by IceCube with a neutrino excess at the 3.3σ level together with three other sources, is similar to the first plausible non-stellar neutrino source, TXS 0506+056, in being also a masquerading BL Lac object, i.e., intrinsically a flat-spectrum radio quasar with hidden broad lines and a standard accretion disk. We point out that these two sources share other properties, including spectral energy distribution, high powers, parsec scale properties, and possibly radio morphology. We speculate that the relatively rare combination of proton-loaded jets, possibly typical of high-excitation sources, and efficient particle acceleration processes, related to their relatively high synchrotron peak frequencies, might favour neutrino production in these two sources. GB6 J1542+6129, which has also recently appeared twice in a list of IceCube associations, seems also to belong to this rare blazar sub-class, which includes at most ≈ 20 *Fermi*-4LAC blazars.

Key words: neutrinos — radiation mechanisms: non-thermal — galaxies: active — BL Lacertae objects: general — radio continuum: galaxies — gamma-rays: galaxies

1 INTRODUCTION

Nine years ago the IceCube Neutrino Observatory¹ detected the first high-energy astrophysical neutrinos of likely extragalactic origin with energies up to > 1 PeV (10^{15} eV) and since then has produced a steady list of events (e.g. Aartsen et al. 2020, and references therein). At present, however, only two astronomical objects have been associated with a significance larger than $\sim 3\sigma$ with these astrophysical neutrinos. Namely, the blazar TXS 0506+056 (IceCube Collaboration et al. 2018a; IceCube Collaboration 2018b) at $z = 0.3365$ and the local ($z = 0.004$) Seyfert 2 galaxy NGC 1068. Aartsen et al. (2020), in fact, have reported on an excess of neutrinos at the 2.9σ level from the direction of NGC 1068 and a 3.3σ excess in the northern sky due to significant p-values in the directions of NGC 1068 and three blazars: TXS 0506+056, PKS 1424+240, and GB6 J1542+6129.

Padovani et al. (2019) showed that TXS 0506+056, despite appearances, is not a blazar of the BL Lac type but instead a masquerading BL Lac object, namely a flat-spectrum radio quasar (FSRQ²) whose

emission lines are swamped by a very bright, Doppler-boosted jet, unlike “real” BL Lacs, which are instead *intrinsically* weak-lined. This is extremely relevant for two reasons: (1) “real” BL Lacs and FSRQs belong to two very different physical classes, i.e., objects *without* and *with* high-excitation emission lines in their optical spectra, referred to as low-excitation (LEGs) and high-excitation galaxies (HEGs), respectively (e.g. Padovani et al. 2017, and references therein); (2) masquerading BL Lacs, being HEGs, benefit from several radiation fields external to the jet (i.e., the accretion disc, photons reprocessed in the broad-line region (BLR) or from the dusty torus), which, by providing more targets for the protons might enhance neutrino production as compared to LEGs.

The aims of this Letter are to: (1) investigate if the second blazar in the Aartsen et al. (2020)’s list, PKS 1424+240, also qualifies as a masquerading BL Lac object; (2) check if TXS 0506+056 and PKS 1424+240 (and GB6 J1542+6129) share other relevant properties. We use a Λ CDM cosmology with Hubble constant $H_0 = 70$ km s⁻¹ Mpc⁻¹, matter density $\Omega_{m,0} = 0.3$, and dark energy density $\Omega_{\Lambda,0} = 0.7$. Spectral indices are defined by $S_\nu \propto \nu^{-\alpha}$ where S_ν is the flux at frequency ν .

* E-mail: ppadovan@eso.org

¹ <http://icecube.wisc.edu>

² Based on optical spectroscopy blazars are classified into FSRQs and BL Lac objects, with the former displaying strong, broad, quasar-like emission lines and the spectra of the latter being often completely featureless and sometimes exhibiting weak absorption and emission lines (e.g. Urry & Padovani 1995).

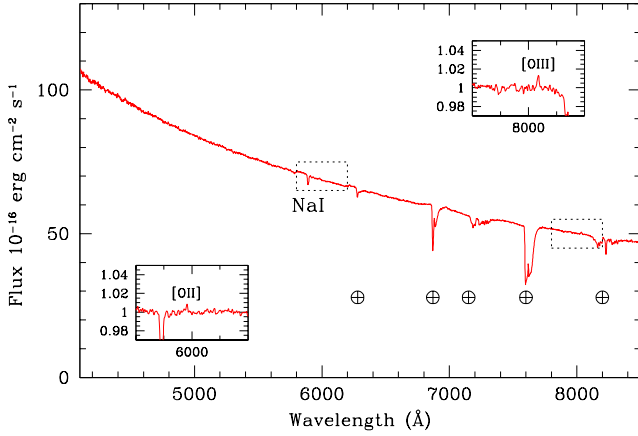


Figure 1. The optical spectrum of PKS 1424+240 obtained at the Gran Telescopio Canarias with the OSIRIS spectrograph (Paiano et al. 2017). The continuum is well described by a power law with spectral index $\alpha = 0.9$ (equivalent to $F_\lambda \propto \lambda^{-1.1}$). Two weak emission lines of [O II] 3727 Å and [O III] 5007 Å (see insets) are detected at $z = 0.6047$. Main telluric lines are indicated by \oplus .

2 THE SOURCE

2.1 Main astronomical data

PKS 1424+240 is one of the most distant TeV-detected blazars, ranked number seven in TeVCat³ at the time of writing, and “a rare example of a luminous HBL⁴” (Cerruti et al. 2017). Its ν_{peak}^S has been estimated to be around $10^{15} - 10^{16}$ Hz, depending on its state (Abdo et al. 2010; Archambault et al. 2014).

The redshift of PKS 1424+240 has a confusing history. The issue has been settled by Paiano et al. (2017), who detected two faint emission lines at 5981 and 8034 Å identified with [O II] 3727 Å and [O III] 5007 Å, with equivalent widths 0.05 and 0.10 Å respectively, at $z = 0.6047$ (Fig. 1). This redshift is also consistent with the presence of a group of galaxies at $z \sim 0.6$ very likely associated with the source (Rovero et al. 2016). These detections imply line powers $L_{[\text{O II}]} \sim 4 \times 10^{41}$ erg s⁻¹ and $L_{[\text{O III}]} \sim 10^{42}$ erg s⁻¹.

As no sign of the host galaxy is apparent in the optical spectrum we cannot decompose it into a non-thermal power law and an elliptical galaxy template to estimate the black hole mass, M_{BH} (e.g. Padovani et al. 2022, hereafter P22; see their Appendix for details). However, we can place an upper limit on $L_{\text{Mg II}} < 5 \times 10^{42}$ erg s⁻¹ assuming this line has a full width at half maximum of 10,000 km s⁻¹. By using eq. (5) and Table 2 of Shaw et al. (2012) we then derive $M_{\text{BH}} < 8 \times 10^8 M_\odot$ (where M_\odot is one solar mass). Note that this is a very robust upper limit, only slightly above the value one would get assuming the host galaxy to be a typical giant elliptical ($M_{\text{BH}} \sim 6.3 \times 10^8 M_\odot$: P22), which translates into an Eddington power $L_{\text{Edd}} < 10^{47}$ erg s⁻¹, with $L_{\text{Edd}} = 1.26 \times 10^{46}$ ($M/10^8 M_\odot$) erg s⁻¹.

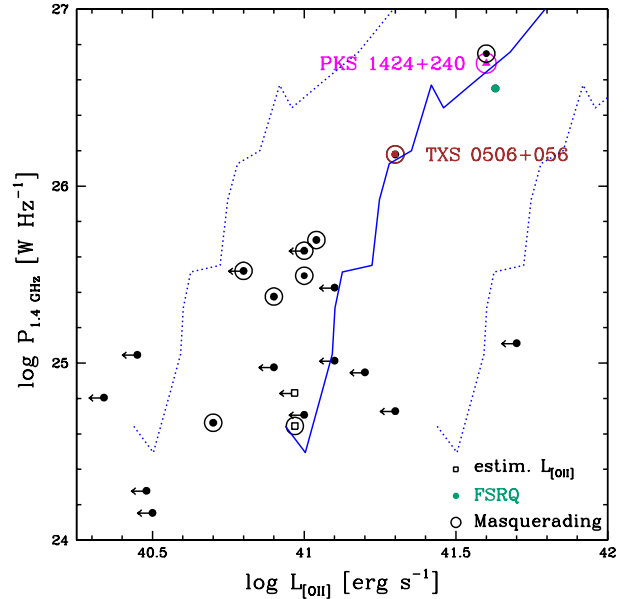


Figure 2. $P_{1.4\text{GHz}}$ vs. $L_{[\text{O II}]}$ for the P22’s sample (black filled circles), with masquerading sources highlighted (larger empty circles). Sources for which $L_{[\text{O II}]}$ has been estimated from $L_{[\text{O III}]}$ are denoted by black empty squares. The magenta triangle is PKS 1424+240, a brown circle indicates TXS 0506+056, while the green filled circle denotes the single FSRQ in the sample. The solid blue line is the locus of jetted (radio-loud) quasars, with the two dotted lines indicating a spread of 0.5 dex, which includes most of the points in Fig. 4 of Kalfountzou et al. (2012). Arrows denote upper limits on $L_{[\text{O II}]}$. Adapted from Fig. 1 of P22.

2.2 Source characterization

We claim that PKS 1424+240 is yet another example of a masquerading BL Lac object linked to IceCube neutrinos. Following Padovani et al. (2019) and P22 this classification is based on four criteria:

(i) its location on the radio power – emission line power, $P_{1.4\text{GHz}} - L_{[\text{O II}]}$, diagram (Fig. 4 of Kalfountzou et al. 2012), which defines the locus of jetted (radio-loud) quasars. With a catalogued 1.4 GHz flux density of 0.43 Jy and a radio spectral index $\alpha_r \sim 0.4$ (NASA/IPAC Extragalactic Database) $P_{1.4\text{GHz}} \sim 5 \times 10^{26}$ W Hz⁻¹, which, together with $L_{[\text{O II}]} \sim 4 \times 10^{41}$ erg s⁻¹, puts this source *exactly* on the locus, as shown by Fig. 2;

(ii) a radio power $P_{1.4\text{GHz}} > 10^{26}$ W Hz⁻¹, typical of HEGs;

(iii) an Eddington ratio $L/L_{\text{Edd}} > 0.03$, hence > 0.01 , which is also one of the defining characteristics of HEGs. This is the ratio between the accretion-related observed luminosity and the Eddington luminosity. The estimation of the former is derived from $L_{[\text{O II}]}$ and $L_{[\text{O III}]}$, as detailed in Padovani et al. (2019). We obtain $L \sim 3 \times 10^{45}$ erg s⁻¹ and a BLR luminosity $L_{\text{BLR}} \sim 10^{44}$ erg s⁻¹;

(iv) a γ -ray Eddington ratio $L_\gamma/L_{\text{Edd}} > 2$ and therefore above the proposed dividing line between “real” BL Lacs and FSRQs (0.1: Sbarrato et al. 2012). In fact, $L_\gamma = 1.7 \times 10^{47}$ erg s⁻¹ (0.1 – 100 GeV), as derived from the *Fermi*-LAT Fourth Source Catalog (4FGL-DR2) energy flux and photon index (Abdollahi et al. 2020; Ballet et al.

³ <http://tevcat.uchicago.edu/>

⁴ Blazars are sub-divided on the basis of the rest-frame frequency of their low-energy (synchrotron) hump (ν_{peak}^S) into low- (LBL/LSP: $\nu_{\text{peak}}^S < 10^{14}$ Hz [< 0.41 eV]), intermediate- (IBL/ISP: 10^{14} Hz $< \nu_{\text{peak}}^S < 10^{15}$ Hz [0.41 – 4.1 eV]), and high-energy (HBL/HSP: $\nu_{\text{peak}}^S > 10^{15}$ Hz [> 4.1 eV]) peaked sources respectively (Padovani & Giommi 1995; Abdo et al. 2010).

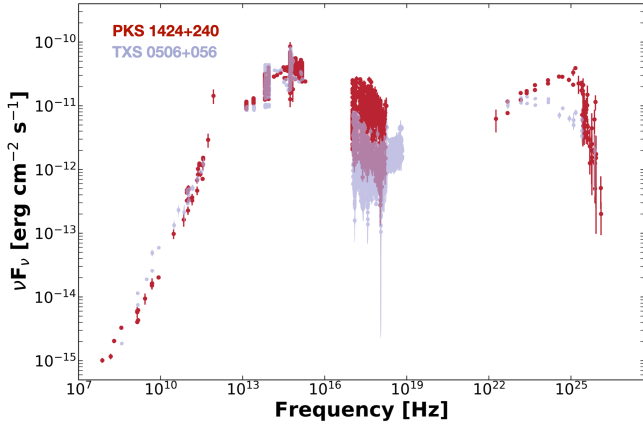


Figure 3. The archival SED of PKS 1424+240 (red points); for comparison the SED of TXS 0506+056 is overlaid (light grey points). The overall SEDs of the two sources are quite similar.

2020). We stress that, due to its very large L_γ , PKS 1424+240 falls outside the boundaries of Fig. 2 of P22 (the $L_\gamma - P_{1.4\text{GHz}}$ plot) and is quite extreme in terms of its location in Fig. 3 (the $\nu_{\text{peak}}^S - L_\gamma$ plot) in the same paper.

In short, PKS 1424+240 meets *all* the above criteria to be classified as a masquerading BL Lac object.

2.3 Similarities between PKS 1424+240 and TXS 0506+056

Apart from being both masquerading BL Lacs, there are quite a few other commonalities between PKS 1424+240 and TXS 0506+056, which make them somewhat special and unusual blazars. Namely:

(i) they are both very powerful IBLs/HBLs, as TXS 0506+056 has $P_{1.4\text{GHz}} \sim 1.5 \times 10^{26} \text{ W Hz}^{-1}$ and $L_\gamma \sim 2.9 \times 10^{46} \text{ erg s}^{-1}$, $\sim 3 - 6$ times smaller than the PKS 1424+240 values;

(ii) the overall SEDs of the two sources are quite similar, both in normalisation and shape. This is clear from Fig. 3, which shows the SED of PKS 1424+240 (red) together with that of TXS 0506+056 (grey). The low-energy parts of the SEDs are almost identical, while there are some difference in the X-ray and γ -ray bands, mostly because of the higher average ν_{peak}^S of PKS 1424+240;

(iii) their parsec scale properties, inferred from Very Long Baseline Interferometry (VLBI) studies, are much more typical of HBLs than of FSRQs. The observed brightness temperature of the centimetre-VLBI core, T_B , is in both cases relatively low, with median values $\sim 6 \times 10^{10} \text{ K}$ in PKS 1424+240 and $\sim 7 \times 10^{10} \text{ K}$ in TXS 0506+056 (Homan et al. 2021), i.e. close to the equipartition value ($\sim 5 \times 10^{10} \text{ K}$; Readhead 1994) and therefore indicative of a modest Doppler boosting. This is also supported by proper motion measurements, revealing low apparent speeds of $v_{\text{app}}/c \equiv \beta_{\text{app}} = 2.83 \pm 0.89$ (Lister et al. 2019) and 1.07 ± 0.14 (Lister et al. 2021) for PKS 1424+240 and TXS 0506+056 respectively. FSRQs, especially the γ -ray powerful ones, are instead characterized by median core T_B approaching and often exceeding the inverse Compton catastrophe limit⁵ due to strong Doppler boosting (Kovalev et al. 2009), as well as by much higher maximum apparent speeds ($\beta_{\text{app}} \sim 10 - 30$,

⁵ The inverse Compton catastrophe is the rapid cooling through inverse Compton scattering of a synchrotron-emitting region, which implies a threshold temperature $\sim 10^{12} \text{ K}$ (Kellermann, Pauliny-Toth, & Williams 1969).

e.g. Jorstad et al. 2017). Homan et al. (2021) estimate relatively low Doppler and Lorentz factors, $\delta \sim 1.8$ and $\Gamma \sim 1.5$ for TXS 0506+056, and $\delta \sim 1.4$ and $\Gamma \sim 4$ and for PKS 1424+240, as typically found for HBLs (Piner & Edwards 2018, and references therein).⁶ A relatively low Lorentz factor is also consistent with the large apparent jet opening angles in both sources (28° and 65° for TXS 0506+056 and PKS 1424+240, respectively, above the median value of 22.6° found for the γ -ray sources in the MOJAVE sample, see Pushkarev et al. 2017). Indeed, the intrinsic aperture of the boosting cone is found to be inversely proportional to Γ , meaning that slower jets will appear less collimated. In conclusion, although these two sources have a standard (Shakura - Sunyaev) disk, as FSRQs, the VLBI properties of their jets are *not* FSRQ-like;

(iv) their extended radio power, P_{ext} , is relatively high, placing the sources in an intermediate regime between Fanaroff-Riley (FR) I and II objects (Fanaroff & Riley 1974), or rather closer to the FRII range ($\log P_{\text{ext}} \gtrsim 25.5 \text{ W Hz}^{-1}$ at 1.4 GHz). Very Large Array (VLA) imaging of PKS 1424+240 at 1.4 GHz reveals a symmetric two-sided structure, with an extended flux density $\sim 130 \text{ mJy}$ (Fig. 12, Rector, Gabuzda, & Stocke 2003), which implies $\log P_{\text{ext}} = 26.3 \text{ W Hz}^{-1}$ ($\alpha = 0.8$), at the lower end of FRII sources. No extended radio emission has been resolved in TXS 0506+056 on kiloparsec (kpc) scales, but an estimate of the extended radio flux density can be obtained by comparing VLBI data with almost contemporaneous single-dish measurements obtained with the Owens Valley Radio Observatory telescope. Li et al. (2020) have shown that the extended emission contributes between 1 and 18 per cent of the total, from which, since the smallest percentage is tied to the largest total flux density (and viceversa), we estimate an extended flux density in the range $15 - 54 \text{ mJy}$ i.e. $\approx 35 \text{ mJy}$ at 15 GHz. This implies $\log P_{\text{ext}} = 25.9_{-0.4}^{+0.2} \text{ W Hz}^{-1}$ at 1.4 GHz for $\alpha = 0.8$, which is close to the FRI/FRII break. Sources classified as BL Lacs but showing intermediate or FRII-like extended radio powers and morphologies are common among bright blazar samples (Rector & Stocke 2001; Kharb, Lister, & Cooper 2010). However, this is mainly true for LBLs, while the properties of HBLs match those of their expected parent population, the FRI radio galaxies (Rector & Stocke 2001; Giroletti et al. 2004). For example, the HBLs in the Einstein Extended Medium Sensitivity Survey, characterised by $0.045 \leq z \leq 0.638$ ($\langle z \rangle \sim 0.3$), have $\log P_{\text{ext}} \sim 23.7$ (and ≤ 25) W Hz^{-1} at 1.4 GHz (Rector & Stocke 2001). Therefore, PKS 1424+240 and TXS 0506+056 appear to be rare examples of IBLs/HBLs with FRII-like radio powers. If the extended radio power is a good proxy of the total jet power (e.g. Willott et al. 1999), the latter should also be in the FRII regime. High jet powers $\sim 10^{45} - 10^{46} \text{ erg s}^{-1}$ are also derived for both sources based on SED modeling (e.g. Aleksić et al. 2014; Ansoldi et al. 2018), much larger than the values, for example, of the low-redshift HBLs MKN 421 and MKN 501 ($\sim 6 \times 10^{43} \text{ erg s}^{-1}$; Potter & Cotter 2015);

(v) the issue of the radio morphology is, instead, difficult to address. TXS 0506+056 is unresolved on kpc scales but the properties of the VLBI jet may be consistent with the development of an FRI morphology. In fact, the rapid increase of the jet opening angle with distance observed in VLBI images at 43 GHz has been interpreted by Ros et al. (2020) as possible evidence for jet deceleration taking place at $\sim 70 - 140 \text{ pc}$ from the BH, a process known to lead to the

⁶ Homan et al. (2021) derive δ by assuming that all sources have the same intrinsic median brightness temperature equal to the sample median, $T_{B,\text{int}} = 10^{10.609 \pm 0.067} \text{ K}$; hence $\delta = T_{B,\text{obs}}/T_{B,\text{int}}$. This population-wide approach, while good for average values, might not be the most appropriate one for individual sources.

formation of an FRI jet (Laing & Bridle 2014). The VLA image of PKS 1424+240 shown by Rector, Gabuzda, & Stocke (2003) presents mixed features, which would need to be better examined at higher resolution: the structure is reminiscent of an edge-brightened FRII, but the rough symmetry of the two-sided jet may be indicative of deceleration as observed in FRIs. In conclusion, one interesting possibility that needs to be further explored is the fact that PKS 1424+240 and TXS 0506+056 might belong to the rare class of efficiently accreting sources, which develop an FRI jet morphology, i.e., FRI-HEGs (e.g. Heckman & Best 2014). A sample of 1.4 GHz selected extended radio sources from the Sloan Digital Sky Survey with $0.03 < z < 0.1$ contains, for example, only 5/245, i.e. 2 per cent, of FRI-HEGs (Miraghaei & Best 2017). Even if that were the case, however, these would have to be sources with FRI morphology and FRII-like jet powers, as discussed above.

2.4 GB6J1542+6129

IceCube Collaboration et al. (2021) have performed a search for flare neutrino emission in the 10 years of IceCube data and reported a cumulative time-dependent neutrino excess in the northern hemisphere at the 3σ level associated with only four sources: a radio galaxy, M87, two blazars, TXS 0506+056 and GB6J1542+6129, and the Seyfert 2 galaxy NGC 1068, these last three sources being also associated with neutrinos by Aartsen et al. (2020). GB6J1542+6129, an IBL (Giommi & Padovani 2021), has then appeared twice in two years in a list of $3 - 3.3\sigma$ IceCube associations and is therefore also worth investigating. The redshift of this object is not available: all we know is that $0.34 \leq z \leq 1.76$ (Shaw et al. 2013), which translates into $P_{1.4\text{GHz}} = 10^{26.4 \pm 0.7} \text{ W Hz}^{-1}$ and $L_\gamma/L_{\text{Edd}} = 10^{0.3 \pm 0.9}$ (for $M_{\text{BH}} = 6.3 \times 10^8 M_\odot$, i.e. assuming the host galaxy to be a typical giant elliptical: Section 2.1). Both values are perfectly consistent with a masquerading BL Lac classification (Section 2.2). From the data given by Homan et al. (2021) we derive $T_{\text{B}} = 1.7 - 3.6 \times 10^{11} \text{ K}$, $\beta_{\text{app}} = 0.8 - 3.1$, $\delta = 4.2 - 8.7$, and $\Gamma = 2.3 - 5.0$ for the adopted redshift range. δ and Γ are therefore also relatively small, which suggests that GB6J1542+6129 shares similar radio properties with the other two sources.

3 DISCUSSION AND SUMMARY

The properties just described highlight the peculiarities of PKS 1424+240 and TXS 0506+056, which may be relevant in the context of neutrino emission models. In particular, a fundamental question concerns the jet particle composition, since the emission of neutrinos requires the presence of relativistic protons. The loading of heavy particles in the jet may occur either in the jet formation process or during jet propagation, as a consequence of entrainment of gas and stars from the environment. Jets formed through the Blandford-Znajek mechanism (Blandford & Znajek 1977) are thought to be light, being mainly composed by electron-positron pairs, while disk-launched jets (e.g. Blandford & Payne 1982) are directly loaded with disk material, and are likely to be heavier and slower (see also Hawley & Krolik 2006; McKinney 2006; Broderick & Tchekhovskoy 2015). If both mechanisms take place at the same time in the AGN, mass exchange, possibly favoured by the development of magneto-hydrodynamic instabilities, may occur between the central relativistic jet and the surrounding heavy disk wind (see e.g. the discussion by Sikora, Stawarz, & Lasota 2007). Mixing and entrainment of heavy particles from the ambient medium are also possible, particularly on larger scales when a jet decelerates and disrupts. Indeed, Croston,

Ineson, & Hardcastle (2018) were able to constrain the composition of the radio-lobe plasma in samples of FRI and FRII sources, showing that the decelerating jets in FRIs require a stronger proton content with respect to FRIIs. These authors also showed that this phenomenon is independent of the AGN accretion mode, being strictly related to the strong interplay between the jet and the environment, which characterizes FRI sources.

However, the most energetic phenomena in the jet, leading to the production of γ -rays up to the TeV regime, are known to occur at smaller distances from the BH, on sub-parsec and parsec scales (e.g. Madejski & Sikora 2016, and references therein). Therefore, it is the jet composition closer to the central engine that may be most relevant in relation to neutrino production. Contrary to the scenario described above for the larger scales, modeling of the jet broadband emission (Celotti & Fabian 1993; Sikora et al. 2005) and observational studies of the jet circular polarization (Homan et al. 2009) suggest that the dynamics of powerful jets is dominated by protons on VLBI scales. The parsec scale properties of the FRI jet in the LEG M 87, on the other hand, are consistent with the dominance of a pair plasma (Reynolds et al. 1996; Broderick & Tchekhovskoy 2015) and, in general, the assumption of light jets appears adequate for the modeling of jet deceleration in FRIs (Laing & Bridle 2002, 2014). This possible difference in the jet composition may reflect a difference in the jet formation mechanism in LEGs (FRIs and FRIIs) and HEGs (mostly FRIIs and a few FRIs). Based on the analysis of the jet collimation profiles, Boccardi et al. (2021) have suggested that a more extended and prominent disk wind surrounds the relativistic spine in HEGs, while the jet expansion profiles in most LEGs are consistent with a jet origin in the vicinity of the ergosphere, as directly observed in M 87. These results support the idea that jets in HEGs are more heavily loaded with protons on sub-parsec and parsec scales.

It then follows that the production of neutrinos might be favoured in sources like PKS 1424+240 and TXS 0506+056. If jets produced by HEGs are indeed more heavily loaded with protons, and if protons and electrons are accelerated in the same regions and through the same mechanisms, then jets from IBL/HBL-HEGs may be those where the two conditions necessary for neutrino production are best met. Namely: 1) a high proton loading; 2) the occurrence of extremely efficient particle acceleration processes. In this scenario FS-RQs would not fulfil the second requirement. In addition, as we mentioned above, the contribution from several external radiation fields typical of HEGs might further enhance neutrino production in these masquerading BL Lac objects.

Any physical mechanism, which may be invoked to explain the emission up to TeV energies in PKS 1424+240 and TXS 0506+056 will have to be reconciled, however, with the low Γ and δ factors observed on parsec scales. Most solutions to the so-called *Doppler factor crisis* have been proposed so far for the case of “classic” low-power HBLs. These include the near-core decelerating jet models (Piner & Edwards 2004, and references therein) and the shock-in-jet models, in which the low apparent speeds are proposed to reflect the formation of quasi-stationary shocks in the jet (Hervet, Boisson, & Sol 2016, and references therein). It is a subject for future investigation whether such solutions are also applicable to the case of the high-power jets in PKS 1424+240 and TXS 0506+056.

In summary, PKS 1424+240, as TXS 0506+056, is another example of a masquerading BL Lac object associated with an IceCube neutrino excess. The two sources share also other properties, including spectral energy distribution, high powers, parsec scale properties, and possibly radio morphology. We suggest that the combination of proton-loaded jets, which might be typical of high-excitation sources, and efficient particle acceleration, implied by their relatively high

synchrotron peak frequencies, might favour neutrino production. Finally, we note that GB6J1542+6129, which has been also recently associated to neutrinos, seems also to belong to this very rare blazar sub-class, although a redshift determination would help to confirm this.

Based on their very high radio and γ -ray powers we estimate that similar sources make up only 2.1 per cent of the total IBL and HBL population⁷. Since IBLs plus HBLs comprise ~ 42 per cent of the *Fermi*-4LAC (clean sample) blazars with SED classification (Ajello et al. 2020; Lott, Gasparrini, & Ciprini 2020), blazars of the type IceCube has associated with neutrinos constitute *at most* 1 per cent of the γ -ray selected population ($\lesssim 20$ sources), since we have not included in our calculation their other peculiar properties.

ACKNOWLEDGMENTS

We thank Maria Petropoulou for her comments on the paper. This work is supported by the Deutsche Forschungsgemeinschaft through grant SFB 1258 “Neutrinos and Dark Matter in Astro- and Particle Physics”.

DATA AVAILABILITY

The flux-calibrated and de-reddened spectrum is available in the on-line database ZBLAC (<http://web.oapd.inaf.it/zblac/>).

REFERENCES

- Aartsen M. G., Ackermann M., Adams J., Aguilar J. A., Ahlers M., Ahrens M., Alispach C., et al., 2020, *PhRvL*, 124, 051103
- Abdo A. A., Ackermann M., Ajello M., et al., 2010, *ApJ*, 716, 30
- Abdollahi S., Acero F., Ackermann M., Ajello M., Atwood W. B., Axelsson M., Baldini L., et al., 2020, *ApJS*, 247, 33
- Ajello M., Angioni R., Axelsson M., Ballet J., Barbiellini G., Bastieri D., Becerra Gonzalez J., et al., 2020, *ApJ*, 892, 105
- Aleksić J., Ansoldi S., Antonelli L. A., Antoranz P., Babic A., Bangale P., Barres de Almeida U., et al., 2014, *A&A*, 567, A135
- Ansoldi S., Antonelli L. A., Arcaro C., Baack D., Babić A., Banerjee B., Bangale P., et al., 2018, *ApJL*, 863, L10
- Archambault S., Aune T., Behera B., Beilicke M., Benbow W., Berger K., Bird R., et al., 2014, *ApJL*, 785, L16
- Ballet J., Burnett T. H., Digel S. W., Lott B., *The Fermi-LAT Collaboration*, 2020, *arXiv:2005.11208*
- Blandford R. D., Znajek R. L., 1977, *MNRAS*, 179, 433
- Blandford R. D., Payne D. G., 1982, *MNRAS*, 199, 883
- Boccardi B., Perucho M., Casadio C., Grandi P., Macconi D., Torresi E., Pellegrini S., et al., 2021, *A&A*, 647, A67
- Broderick A. E., Tchekhovskoy A., 2015, *ApJ*, 809, 97
- Celotti A., Fabian A. C., 1993, *MNRAS*, 264, 228
- Cerruti M., Benbow W., Chen X., Dumm J. P., Fortson L. F., Shahinyan K., 2017, *A&A*, 606, A68
- Croston J. H., Ineson J., Hardcastle M. J., 2018, *MNRAS*, 476, 1614
- Fanaroff B. L., Riley J. M., 1974, *MNRAS*, 167, 31P
- Ghisellini G., Tavecchio F., Chiaberge M., 2005, *A&A*, 432, 401
- Giommi P., Padovani P., 2021, *Universe*, 7(12), 492
- Giroletti M., Giovannini G., Taylor G. B., Falomo R., 2004, *ApJ*, 613, 752
- Hardcastle M. J., Croston J. H., 2020, *NewAR*, 88, 101539
- Hawley J. F., Krolik J. H., 2006, *ApJ*, 641, 103
- Heckman T. M., Best P. N., 2014, *ARA&A*, 52, 589
- Hervet O., Boisson C., Sol H., 2016, *A&A*, 592, A22
- Homan D. C., Lister M. L., Aller H. D., Aller M. F., Wardle J. F. C., 2009, *ApJ*, 696, 328
- Homan D. C., Cohen M. H., Hovatta T., Kellermann K. I., Kovalev Y. Y., Lister M. L., Popkov A. V., et al., 2021, *ApJ*, in press (*arXiv:2109.04977*)
- IceCube Collaboration, 2018, *Science*, 361, 147
- IceCube Collaboration et al., 2018, *Science*, 361, eaat1378
- IceCube Collaboration, Abbasi R., Ackermann M., Adams J., Aguilar J. A., Ahlers M., Ahrens M., Alispach C., et al., 2021, *ApJL*, 920, L45
- Jorstad S. G., Marscher A. P., Morozova D. A., Troitsky I. S., Agudo I., Casadio C., Foord A., et al., 2017, *ApJ*, 846, 98
- Kalfountzou E., Jarvis M. J., Bonfield D. G., Hardcastle M. J., 2012, *MNRAS*, 427, 2401
- Kellermann K. I., Pauliny-Toth I. I. K., Williams P. J. S., 1969, *ApJ*, 157, 1
- Kharb P., Lister M. L., Cooper N. J., 2010, *ApJ*, 710, 764
- Kovalev Y. Y., Aller H. D., Aller M. F., Homan D. C., Kadler M., Kellermann K. I., Kovalev Y. A., et al., 2009, *ApJL*, 696, L17
- Laing R. A., Bridle A. H., 2002, *MNRAS*, 336, 1161
- Laing R. A., Bridle A. H., 2014, *MNRAS*, 437, 3405
- Li X., An T., Mohan P., Giroletti M., 2020, *ApJ*, 896, 63
- Lister M. L., Homan D. C., Hovatta T., Kellermann K. I., Kiehlmann S., Kovalev Y. Y., Max-Moerbeck W., et al., 2019, *ApJ*, 874, 43
- Lister M. L., Homan D. C., Kellermann K. I., Kovalev Y. Y., Pushkarev A. B., Ros, E., Savolainen, T., 2021, *ApJ*, in press (*arXiv:2108.13358*)
- Lott B., Gasparrini D., Ciprini S., 2020, *arXiv:2010.08406*
- Madejski G., Sikora M., 2016, *ARA&A*, 54, 725
- McKinney J. C., 2006, *MNRAS*, 368, 1561
- Miraghaei H., Best P. N., 2017, *MNRAS*, 466, 4346
- Padovani P., Giommi P., 1995, *ApJ*, 444, 567
- Padovani P., et al., 2017, *A&AR*, 25, 2
- Padovani P., Oikonomou F., Petropoulou M., Giommi P., Resconi E., 2019, *MNRAS*, 484, L104
- Padovani P., Giommi P., Falomo R., Oikonomou F., Petropoulou M., Glauch T., Resconi E., Treves A., Paiano S., 2022, *MNRAS*, 510, 2671 (P22)
- Paiano S., Landoni M., Falomo R., Treves A., Scarpa R., Righi C., 2017, *ApJ*, 837, 144
- Piner B. G., Edwards P. G., 2004, *ApJ*, 600, 115
- Piner B. G., Edwards P. G., 2018, *ApJ*, 853, 68
- Potter W. J., Cotter G., 2015, *MNRAS*, 453, 4070
- Pushkarev A. B., Kovalev Y. Y., Lister M. L., Savolainen T., 2017, *MNRAS*, 468, 4992
- Readhead A. C. S., 1994, *ApJ*, 426, 51
- Rector T. A., Stocke J. T., 2001, *AJ*, 122, 565
- Rector T. A., Gabuzda D. C., Stocke J. T., 2003, *AJ*, 125, 1060
- Reynolds C. S., Fabian A. C., Celotti A., Rees M. J., 1996, *MNRAS*, 283, 873
- Ros E., Kadler M., Perucho M., Boccardi B., Cao H.-M., Giroletti M., Krauß F., et al., 2020, *A&A*, 633, L1
- Rovero A. C., Muriel H., Donzelli C., Pichel A., 2016, *A&A*, 589, A92
- Sbarrato T., Ghisellini G., Maraschi L., Colpi M., 2012, *MNRAS*, 421, 1764
- Shaw M. S., Romani R. W., Cotter G., Healey S. E., Michelson P. F., Readhead A. C. S., Richards J. L., et al., 2012, *ApJ*, 748, 49
- Shaw M. S., Romani R. W., Cotter G., Healey S. E., Michelson P. F., Readhead A. C. S., Richards J. L., et al., 2013, *ApJ*, 764, 135
- Sikora M., Begelman M. C., Madejski G. M., Lasota J.-P., 2005, *ApJ*, 625, 72
- Sikora M., Stawarz Ł., Lasota J.-P., 2007, *ApJ*, 658, 815
- Urry C. M., Padovani P., 1995, *PASP*, 107, 803
- Willott C. J., Rawlings S., Blundell K. M., Lacy M., 1999, *MNRAS*, 309, 1017

⁷ This is the fraction of sources with radio and γ -ray powers larger than those of TXS 0506+056 in the IBL/HBL sample put together by Giommi & Padovani (2021). GB6J1542+6129 has $P_{1.4\text{GHz}} = 10^{26.4\pm 0.7} \text{ W Hz}^{-1}$ and $L_{\gamma} = 10^{47.2\pm 0.9} \text{ erg s}^{-1}$.

This paper has been typeset from a \LaTeX file prepared by the author.